
# Neural network-assisted decision-making for adaptive routing strategy in optical datacenter networks

Optical Switching and Networking 45 (2022) 100677

Contents lists available at ScienceDirect

Optical Switching and Networking

journal homepage: www.elsevier.com/locate/osn

# Neural network-assisted decision-making for adaptive routing strategy in optical datacenter networks

Yuanyuan Hong [a], Xuezhi Hong [b,*], Jiajia Chen [c,**]

[a] School of Electronics and Information Engineering, Taizhou University, Taizhou, 318000, China
[b] ZJU-SCNU Joint Research Center of Photonics, South China Normal University, Guangzhou, 510631, China
[c] Chalmers University of Technology, Gothenburg, 41296, Sweden

ARTICLE INFO

*INDEX TERMS:*
Datacenter network (DCN)
Neural network (NN)
Optical interconnect
Routing and spectrum allocation (RSA)

ABSTRACT

To improve the blocking probability (BP) performance and enhance the resource utilization, a correct decision of routing strategy which is most adaptable to the network configuration and traffic dynamics is essential for adaptive routing in optical datacenter networks (DCNs). A neural network (NN)-assisted decision-making scheme is proposed to find the optimal routing strategy in optical DCNs by predicting the BP performance for various candidate routing strategies. The features of an optical DCN architecture (i.e., the rack number *N*, connection degree *D*, spectral slot number *S* and optical transceiver number *M*) and the traffic pattern (i.e., the ratio of requests of various capacities *R*, and the load of arriving request) are used as the input to the NN to estimate the optimal routing strategy. A case of two-strategy decision in the transparent optical multi-hop interconnected DCN is studied. Three metrics are defined for performance evaluation, which include (a) the ratio of the load range with wrong decision over the whole load range of interest (i.e., decision error *E*), (b) the maximum BP loss (*BPL*) and (c) the resource utilization loss (*UL*) caused by the wrong decision. Numerical results show that the ratio of error-free cases over tested cases always surpasses 83% and the average values of *E*, *BPL* and *UL* are less than 3.0%, 4.0% and 1.2%, respectively, which implies the high accuracy of the proposed scheme. The results validate the feasibility of the proposed scheme which facilitates the autonomous implementation of adaptive routing in optical DCNs.

## 1. Introduction

According to the Cisco forecast, the global data center traffic will reach 20.6 Zettabytes by the end of 2021 with a compound annual growth rate of 25% [1]. Such a significant traffic growth poses great challenges in datacenter networks (DCNs), which calls for research to support continuously increasing capacity while satisfying the indispensable requirement in power consumption [2,3]. The optical interconnect has been widely considered as a promising solution for DCNs as it can achieve larger capacity and higher power efficiency than its electrical counterparts by the researchers and large enterprises [3–6]. Various optical interconnects architectures have been proposed to explore the above advantages to benefit DCNs [3,7–11]. Nevertheless, since the port number of the optical switches in general is much smaller than that of the electronic ones, efficient routing schemes become essential for optical DCNs to achieve the all-to-all connections with low blocking probabilities. In this regard, intensive research efforts have been made on the optimization of routing for the arriving requests to improve the network performance of optical DCNs [12–15]. Dynamic routing for the anycast and unicast traffics in the inter-datacenter optical networks has been demonstrated [12,13]. Survivable routing, spectrum and waveband assignment strategy in the cloud optical and data center networks have been studied in Ref. [14]. Besides the routing methods that leverage flexible modulation format conversion and spectrum fragmentation in Refs. [12–14], adaptive routing has been proposed to improve the utilization of the spectrum and optical transceivers under the resource deficiency [15]. With the adaptive routing scheme, the blocking probability of optical DCN can be decreased by up to one order when compared with the non-adaptive routing schemes [15]. Nevertheless, such an advantage of adaptive routing relies on the correct decision of the optimal routing strategy which is most adaptable to the network configuration and traffic dynamics. Traditionally the optimal

* Corresponding author.
** Corresponding author.
*E-mail addresses:* xuezhi.hong@coer-scnu.org (X. Hong), jiajiac@chalmers.se (J. Chen).

https://doi.org/10.1016/j.osn.2022.100677
Received 7 July 2021; Received in revised form 13 February 2022; Accepted 18 April 2022
Available online 21 April 2022

routing strategies (e.g., strategies based on specific cost functions [15]), for different networks are selected based on the network operators' experience. Once they are selected, they would not be changed even if the traffic situation or network configurations are varied. This may result in low efficiency and limit the performance of optical DCNs.

On the other hand, machine learning (ML) algorithms have been introduced for the routing of optical networks to improve the efficiency of resource utilization and the network performance. S. Troia et al. [16] established the multi-layer optimization model which finds the optimal routing and wavelength assignment and virtual network function (VNF) arrangement as the environment for the Reinforcement Learning (RL) system for the dynamic resources allocation in the metro-core optical networks. I. Martin et al. [17] proposed the ML-based routing and wavelength assignment for the input traffic matrix in the optical wavelength division multiplexing (WDM) network. X. Chen et al. [18] proposed the cognitive routing, modulation format and spectrum assignment agent in the elastic optical networks based on the deep-reinforcement-learning approach, which improves the BP performance. L. Li et al. [19] chose the optimal path for the circuit-switched networks based on the prediction of the blocking probability (BP) performance of all candidate paths with a naive Bayesian classifier. However, these ML-based works focus on conventional telecommunication networks, and may not be directly applicable for the routing tasks in optical DCNs, which often have high complexity of traffic situation.

The optical DCNs have to work with various network segments (e.g., the long-reach backbone network and the wireless sensor network, etc.) to support the rapidly growing applications like 5G, Internet of Things (IoT), etc. The transmission performance, the network configuration and the service requirement of these segments differ significantly. Furthermore, the optical interconnect architectures, particularly for large-scale DCNs, usually need to be highly scalable to satisfy the surging demands of data computation, storage and communication [8,10,20,21]. Besides, the traffic at the optical DCNs experiences the bursty temporal and spatial variation [22,23]. The features of the optical DCNs in terms of heterogeneity, scalability and traffic dynamics lead to the high complexity in path provisioning. The traditional routing methods based on pre-engineered static principles have difficulty in dealing with such challenges. Smart decision-making scheme of routing with the assistance of ML technologies is able to improve the decision accuracy and efficiency. W. Liu et al. [24,25] proposed the deep reinforcement learning-based routing (DRL-R), making a choice of the candidate paths for each arriving request to optimize the resource efficiency and network performance. X. Chen et al. [26] presented the knowledge-based autonomous service provisioning framework, where ML technology is used to realize the quality-of-transmission (QoT)-aware inter-domain path provisioning. In their work, the most cost-effective light path is set up while the QoT is guaranteed with the predicted bit error rate of the candidate paths. Both the frameworks were designed for provisioning the optimal decision for every candidate path.

In this paper, we propose a neural network (NN) assisted decision-making scheme to select the optimal routing strategy instead of the optical routing path, which facilitates the adaptive routing in optical DCNs from a new perspective. The decision of the optimal routing strategy is made based on the predicted network performance by the trained NN model, where the corresponding load of arriving requests and configurations of optical DCNs are given. To better identify the characteristic of the proposed decision-making scheme under the dynamic nature of DCN traffic, the performance of the scheme should be analyzed over a range of traffic load rather than the certain traffic load. Therefore, three metrics, i.e., the decision error which is defined as the ratio of wrong decision range over the whole range of interest in terms of traffic load, and the maximum losses of BP and resource utilization within the whole traffic load range of interest, are proposed to quantify the performance of the proposed scheme. Numerical results show that error-free decision-making is achieved in a large portion of tested cases covering the overall observed traffic load range and different network parameters, resulting in low average decision error and network performance degradation in terms of BP and resource utilization.

The remainder of the paper is organized as follows. Section II illustrates the proposed NN-assisted decision-making scheme to select the routing strategy in the optical DCNs as well as the studied use case of the decision-making between two routing strategies for the transparent optical multi-hop interconnected DCN. In Section III, the evaluation method which defines the new metrics for quantifying the performance of the proposed scheme is illustrated. Then the impact of observation range and the network parameters on the performance, in terms of the three newly defined metrics, i.e., decision error, the BP loss and resource utilization loss due to the wrong decision, is analyzed based on the observation of all the studied case. Finally, Section IV draws the conclusions.

## 2. NN-assisted decision-making scheme for routing strategy selection in optical datacenter networks

In this section, we first describe the procedure of the proposed NN-assisted decision-making scheme for routing strategy selection in optical DCNs. Then we focus on a use case that involves two candidate routing strategies in the transparent optical multi-hop interconnected DCN [15]. This use case will be further considered in Section III for performance evaluation.

### 2.1. Procedure of NN-assisted decision-making scheme

In adaptive routing, routing strategies that emphasize on different aspects of resource deficiency perform differently in various optical DCNs [15]. The optimal routing strategy that achieves the lowest BP at a certain load of arriving requests is jointly determined by a number of network parameters, including the static parameters of network scale, interconnection configuration, resources (e.g., the spectrum and optical transceivers) deployment, and the dynamic parameters of arriving requests (e.g., the required capacity of arriving requests). To automatically select the optimal strategy for adaptive routing in the optical DCNs, we propose an NN-assisted decision-making scheme.

Fig. 1(a) and (b) describe the flow of the proposed NN-assisted decision-making scheme for adaptive routing. The proposed scheme consists of two phases, i.e., training and provisioning. In the training phase, the data set of BP performance with various routing strategies for different networks and traffic loads is collected from simulation or realistic data from the operators. The NN model configured as Fig. 1(c) is trained with the assembled data set. Once training is completed, the trained NN model is capable of predicting BP performance corresponding to the DCN with any parameter set $X_{Net}$, which contains the interconnection configuration (i.e., the number of ports one rack is connected to of the optical switching matrix), network scale, resources deployment, required capacity of the arriving requests, traffic load $X_{load}$ and candidate routing strategies in the set $C$. In the provisioning phase, the BP performance $BP_c$ corresponding to $X_{load}$ in a DCN with $X_{Net}$ for each candidate routing strategy $c$ is predicted with the trained NN model. The routing strategy that offers the lowest BP is chosen as the optimal strategy $OC$.

### 2.2. Use case

To investigate the proposed NN-assisted decision-making scheme for routing strategy selection, the use case where two candidate routing strategies are considered for selection, referred to as two-strategy decision, and the transparent optical multi-hop interconnected architecture [15] is adopted for DCN. Note that the similar way can also be applied to the cases with the number of routing strategy candidates larger than two for the network performance prediction. The optimal strategy can then be provisioned for adaptive routing. The two strategies which are to be determined in the use case correspond to the adopted different cost

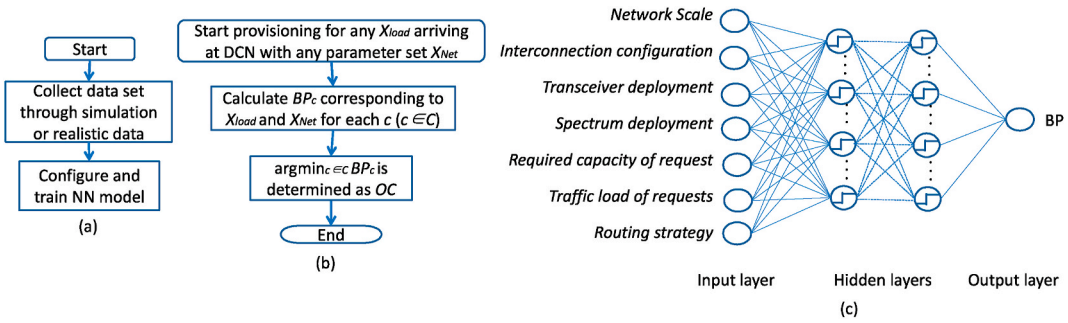


**Fig. 1.** The procedure of NN–assisted decision–making scheme for adaptive routing in optical DCNs: (a) The training phase, and (b) the provisioning phase, and (c) the architecture of the NN model. $X_{load}$ and $X_{Net}$ represent the load of arriving requests and the DCN for which the strategy decision is provisioned, respectively. To be specific, $X_{Net}$ contains the parameters of network scale, interconnection configuration, transceiver and spectrum deployment, required capacity of arriving request, etc. $X_{Net}$, $X_{load}$ and the adopted routing strategy are input to NN for predicting corresponding BP as shown in (c). $C = \{c\}$ is the set of routing strategies, where each element $c$ represents a routing strategy. $OC$ refers to the optimal strategy in $C$ for $X_{load}$ and $X_{Net}$. $BP_c$ represents the predicted blocking probability performance with the routing strategy $c$.

functions of the links. In the investigated DCN architecture in this work, the racks are interconnected through the optical switching matrix (OSM) and the optical multi-hop paths provisioned to satisfy the connection demands are composed of one or several transparent links that connect the rack pairs by passing the OSM and fiber links without any optical-electrical-optical (OEO) conversion at the intermediate racks. It is verified that the interconnection degree ($D$), which indicates the maximum number of racks one rack simultaneously communicates with, has a great impact on the performance of the considered DCN architecture [15]. Therefore, the degree $D$ is set as the interconnection configuration parameter of the studied case and input to the NN for the BP prediction.

Besides $D$, the predicted BP performance also depends on the parameters of network scale, spectrum and number of optical transceivers at each rack, the capacity and the load of arriving connection requests as well as the adopted routing strategy. For the studied DCN, the network scale is characterized by the number of racks $N$. The configurations of spectrum and optical transceivers are indicated by the numbers of spectral slots on each fiber link $S$ and the number of transceivers on each rack $M$, respectively. The dynamic parameters of the arriving connection requests contain not only the load of requests, but also the ratio of requests with various demanded capacities $R$, which determines the average capacity of arriving connection requests. The necessity of inputting $R$ to the NN for BP prediction is due to the diversity of capacity requirements of connection requests (e.g., the mixed 40 Gbps and 100 Gbps capacity requests) arriving at the investigated DCN. The two routing strategies correspond to implementing two different types of link cost function as shown in (1) and (2) [15]. The cost of a transparent link equals the number of fiber links within the transparent link between the rack pair ($i$, $j$), i.e. $Numlink$ ($i$, $j$), or the square of the fiber link number, i.e. ($Numlink$ ($i$, $j$))$^2$. With the second type of link function cost, a longer path has a lower possibility to be selected.

In our studied case, the BP performance is predicted given the network parameters $N$, $D$, $M$, $S$, $R$ and the load as well as the link cost functions (1) and (2). The symbols and the corresponding definitions of the NN input in the case are listed in Table 1.

$$\cos t_1(i,j) = Numlink(i,j), \tag{1}$$

$$\cos t_2(i,j) = (Numlink(i,j))^2. \tag{2}$$

According to the observation of the load-versus-BP performance of the studied DCN cases, the routing strategy with link cost function $\text{cost}_1$ always outperforms that with $\text{cost}_2$ when the load is relatively large, regardless of network parameters. For conciseness, the two candidate routing strategies are denoted as $\text{cost}_1$ and $\text{cost}_2$, respectively. The superiority of the $\text{cost}_1$ over the $\text{cost}_2$ for a large traffic load is attributed to the fact that the $\text{cost}_1$ prefers routes with longer transparent optical paths and less occupation of transceivers, which can be seen from (1) and (2). Nevertheless, when the load is small or medium, the observed optimal routing strategy can be one of these two candidates, which varies at different load values and network parameters.

**Table 1**
Input of the NN in the use case.

| Symbol | Definition |
|---|---|
| $N$ | The number of racks, which refers to the "Network scale" of the NN input in the proposed scheme as shown in Fig. 1(c). |
| $D$ | The maximum number of racks one rack simultaneously communicates with, which refers to the "Interconnection configuration" of the NN input in the proposed scheme as shown in Fig. 1(c). |
| $M$ | The number of transceivers on each rack, which refers to the "Transceiver deployment" of the NN input in the proposed scheme as shown in Fig. 1(c). |
| $S$ | The number of spectral slots on each fiber link, which refers to the "Spectrum deployment" of the NN input in the proposed scheme as shown in Fig. 1(c). |
| $R$ | The ratio of requests with various demanded capacities, i.e. 40 Gbps and 100 Gbps, which determines the average capacity of demanded requests and refers to the "Required capacity of requests" of the NN input in the proposed scheme as shown in Fig. 1(c). |
| $Load$ | This refers to the "Traffic load of requests" of the NN input in the proposed scheme as shown in Fig. 1(c). |
| $Cost$ | The link cost functions (1) and (2), which refers to the "Routing strategy" of the NN input in the proposed scheme as shown in Fig. 1(c). |

It is observed there is at most one intersection of BP-versus-load curves of $\text{cost}_1$ and $\text{cost}_2$ for all the tested cases. The intersection matters in the assessment of the routing decision, i.e., the performance advantage of $\text{cost}_1$ and $\text{cost}_2$ is opposite on different sides of the intersection. To guarantee the quality of service in DCNs, the BP of the network shall be smaller than a certain value that is referred to as the BP threshold $Th_{BP}$. The range of interest in terms of the load is [0, $Th$], where $Th$ indicates the largest one of $Th_i$ with $cost_i$ among all the investigated strategies. In the use case of the two-strategy decision, $i \in$ [1,2]. Depending on the relationship between the range of interest and the intersection, three situations are observed for all tested cases (see Fig. 2).

In the proposed scheme, the BP for each candidate routing strategy is predicted by the NN before the decision of optimal routing strategy is made. Since the BP predicted by the NN in general is not the same as the real BP (i.e., the BP obtained from the real deployment, e.g., from the discrete-event simulator in this study) due to estimation error, the provisioned optimal routing strategy by the NN can be different from the actual one. To facilitate the analysis of the impact of inaccurate prediction from the NN on the performance of adaptive routing, seven scenarios that are collected from all tested cases are listed:

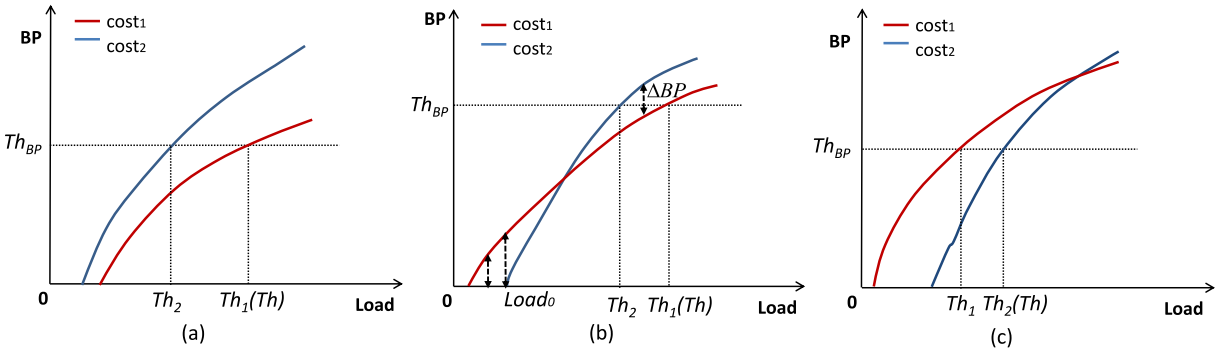


**Fig. 2.** The relationship between the intersection of two routing strategies and the observation range for various situations. For situation (a), there is no intersection in the range of interest. The intersection falls (b) within the observation range and (c) on the right side of the observation range. As an example, the difference of BP performances with the two strategies, i.e. $\Delta BP$, at various load is marked in the situation (b), where $\Delta BP$ first increases and then decreases along with the load rising from zero to the intersection. As the load continues rising, $\Delta BP$ increases with the load. $Th_{BP}$ and $Th$ indicate the worst acceptable BP performance and the corresponding load of requests, respectively. $Th$ equals the larger one of $Th_i$ where $cost_i$ is implemented (i.e. $Th_1$ in situations (a) and (b) and $Th_2$ in (c)) ($i = 1, 2$). $Load_0$ indicates the initialized load when the blocking occurs with $cost_2$.

#### 2.2.1. Scenarios 1 and 7

Both the intersections obtained by the real deployment (i.e. $In_{real}$) and NN prediction method (i.e. $In_{pre}$) are with the situation shown in Fig. 2(a) (Fig. 2(c)) for Scenario 1 (Scenario 7);

#### 2.2.2. Scenario 2

$In_{real}$ is with the situation shown in Fig. 2(a) while $In_{pre}$ is with the situation shown in Fig. 2(b);

#### 2.2.3. Scenarios 4, 5 and 6

$In_{real}$ is with the situation shown in Fig. 2(b) while $In_{pre}$ is with the situations shown in Fig. 2(a), (b) and 2(c) for Scenarios 4, 5 and 6, respectively;

#### 2.2.4. Scenario 3

$In_{real}$ is with the situation shown in Fig. 2(a) while $In_{pre}$ is with the situation shown in Fig. 2(c).

It should be noted that there are still possible scenarios not addressed here, i.e., that the $In_{real}$ is with the situation shown in Fig. 2(c) while $In_{pre}$ is with the situation shown in Fig. 2(a) and (b). These scenarios are observed based on the 243 tested cases, which will be described in Section III. Despite of the finiteness of the studied network samples, it can be clearly seen that the considered Scenarios dominate, particularly for Scenarios 1 and 7.

The detailed calculation of decision error ($E$), maximum BP loss ($BPL$) and resource utilization loss ($UL$) (see definitions in Table 2 of Section III-A) for the seven scenarios is shown in Table 3 of APPENDIX. It should be noted that the accuracy analysis of this work is executed based on the observation from all tested cases, where there is only one intersection of the BP-versus-load curves of $cost_1$ and $cost_2$ and seven scenarios in terms of the relationship between the intersections and the range of interest. In case there are more intersections than that in the above scenarios, the accuracy analysis could be more complicated and should be adapted accordingly, which is left for future research.

## 3. Performance evaluation

In this section, the impacts of observation range and the network parameters $N$, $D$, $M$, $S$ and $R$ on the performance of the studied use case are investigated numerically. In this paper, we use simulation results calculated based on discrete event-driven simulator to represent data for the real deployment as the benchmark for evaluation. Despite of this, we still use the symbol $In_{real}$ to represent the intersection obtained with simulation for consistency with Section II. In case the data of the real deployment is available, the same methodology can be used. To evaluate the performance of various DCNs, we take $D$ as 4, 6, 8, $M$ as 12, 16, 20, $N$ as 32, 64, 96, $R$ as 0.1, 0.5, 0.9 and $S$ as 48, 64, 80, which results in the sample of $3^5 = 243$ network cases. The cumulative distribution function (CDF) of the $E$, $BPL$ and $UL$ of the 243 tested cases together with their distributions over the seven scenarios are measured. The configurations of the NN model and the used data set for training are illustrated as follows.

**Table 2**
Definition of performance metrics and the relevant symbols.

| Symbol | Definition |
|---|---|
| $\{In_{realij}\}$ | The set of load coordinates of the intersections of load-versus-BP performance corresponding to $cost_i$ and $cost_j$ calculated with real deployment. |
| $\{In_{preij}\}$ | The set of NN predicted load coordinates of the intersections of load-versus-BP performance corresponding to $cost_i$ and $cost_j$. |
| $Th$ | The largest load of the range of interest. It can be calculated according to the given largest allowed BP ($Th_{BP}$), i.e., $Th$ equals to the greatest load $Th_i$ at BP = $Th_{BP}$ with $cost_i$ among all the investigated strategies. |
| $Load_{max}$ | The load that maximizes the BP difference among various routing strategies. It corresponds to maximum BP loss and resource utilization loss throughout the range of interest. |
| $E$ | The decision error equals the ratio of wrong decision range over the whole range for decision-making, i.e. [0, $Th$]. |
| $BPL$ | The maximum BP loss caused by the wrong decision-making in the observation range. If the $cost_i$ and $cost_j$ correspond to the best and worst BP performance at a given load, respectively, the $BPL_{load}$ equals to $(BP_j\text{-}BP_i)/BP_j$. The $BPL$ equals the $BPL_{load}$ measured at load = $Load_{max}$. |
| $UL$ | The resource utilization loss caused by the wrong decision-making throughout the observation range. The BP performance of a certain routing strategy can be improved with more resource. The $UL$ quantifies the difference in required resource for a fixed BP for different routing strategies. Suppose $cost_i$ and $cost_j$ result in the best and worst BP performance at certain load, respectively, additional $R_a$ resource units are needed to achieve the same BP if using $cost_j$ instead of $cost_i$. The $UL_{load}$ equals $R_a/(R + R_a)$, where $R$ indicates the number of resource units for $cost_i$. The $UL$ equals the $UL_{load}$ measured at load = $Load_{max}$. |

In the training phase, 952 randomly generated training samples are used for training. Each sample contains the network parameters $N$, $D$, $M$, $S$, $R$, the employed routing strategy, the traffic load, as well as the corresponding BP. The BP performance is evaluated by a homemade discrete event-driven simulator. The arrival and the holding time of the connection requests follow the Poisson and exponential distribution, respectively. The source and destination racks for the connections are uniformly distributed. The arriving connection requests demand two data rates, 40 Gbps and 100 Gbps, to represent the diverse capacity requirements of connections in the optical DCNs. The flex-grid technique is employed with the minimum unit of spectrum slot of 6.25 GHz. The modulation format is set to be 4QAM. To satisfy the connection requests of 40 Gbps and 100 Gbps, the maximum required numbers of

spectrum slots are 4 and 10, respectively. The transmission reach in the datacenter is typically short (usually no larger than 2 km). Due to the intersection losses of the wavelength selective switches WSSs and optical switching matrix OSM, the largest possible number of hops is limited to 3. For the *K*-shortest path algorithm used in the routing scheme, the *K* is set up to 3 [15]. To reflect the scalability and traffic dynamic features in the optical DCN, the network parameters are configured to be varied. According to Ref. [8], there could be dozens of racks, each of which has tens of transceivers. The rack number *N* and optical transceiver number *M* are set to be varied in the ranges of [48–80] and [12–32], respectively. The ratio of 40 Gbps over 100 Gbps connection requests *R* varies in the range of [0.1–0.95]. The number of spectral slots *S* is defined as the ratio of the whole optical spectrum width (several hundreds of GHz in elastic optical networks [27]) over the smallest spectrum slot width, which is set as 6.25 GHz, and thus the *S* is set to vary in the range of [16–128]. We also set the connection degree *D* to be varied in the range of [4–16] and load varied in [20–600]. The BP of each entry is obtained with a confidence level of 90% at 10% interval and over 20,000 requests [15]. Each of the 952 training samples is obtained by the randomly selected parameter set of *N*, *D*, *M*, *S*, *R* and the load varying in the corresponding ranges, and the BP calculated in the specified DCN case with the discrete event-driven simulator.

The parameters of the NN, including the number of hidden layers, the number of neurons in each hidden layer, the activation function of neurons and the learning rate [28], are fine tuned to improve the prediction accuracy. The optimized NN for this study is found to be with two hidden layers and 10 neurons in each layer. The activation function of neurons in each layer is set as the hyperbolic tangent sigmoid function. The learning rate in training is set to be 0.1. To improve the accuracy of BP prediction in the provisioning phase, 100 NNs are trained with the same training data but with different randomly initialized weights and biases. The predicted value of each BP is obtained by averaging the output of all 100 NNs with the same input. In terms of the validation procedure of the NN model, the handout cross validation method [29] that divides the collected samples into the training, validation and test sets and decides when to stop training based on the measured performance on the validation set is employed. The training, validation and test sets are obtained by randomly dividing the collected samples into 7:1.5:1.5. The performance function used for the evaluation is the mean square error (MSE). The training stops once the MSE stops decreasing for 6 continuous epochs.

### 3.1. Evaluation methodology

To better quantify the performance of the NN-assisted strategy decision-making, the new evaluation methodology is proposed. Considering the dynamics of traffic in the optical DCNs, the accuracy of strategy decision is assessed for a range of traffic load rather than a certain value of load. Three metrics are proposed to quantify the accuracy of the proposed scheme and its impact on performance: (a) decision error (*E*) is the range of wrong decision over the whole range of decision-making, (b) maximum BP loss (*BPL*) and (c) resource utilization loss (*UL*) are the losses over the range of interest, respectively. The *BPL* and *UL* correspond to the worst case when assessing the impact of an erroneous strategy decision on the system performance throughout the observation range. The definitions of *E*, *BPL* and *UL* as well as the definitions of the used symbols for calculating them are listed in Table 2. For any network case with a certain parameter set {*N*, *D*, *M*, *S*, *R*}, *E*, *BPL* and *UL* can be calculated according to the definitions in Table 2.

As described before, the investigated two-strategy decision use cases can be categorized as seven scenarios according to the relationship between the range of interest and the intersection. To better explain the evaluation methodology, the calculation of *E*, *BPL* and *UL* for the DCN cases of the seven scenarios is shown in Table 3 in APPENDIX. For Scenarios 1 and 7, error-free decision is achieved (i.e., *E, BPL* and *UL* equal 0). This is because there is no intersection in the range of interest [0, *Th*]. The $cost_1$ ($cost_2$) is determined as the optimal cost for any load in the range of interest. On contrary, though no intersection exists in the range of interest for Scenarios 3, the preferred routing strategy obtained with the NN assisted decision-making is opposite with that obtained by the simulation in the whole observation range (i.e., *E* equals 1). For Scenarios 2, 4, 5 and 6, *E* falls between 0 and 1 and can be calculated based on its definition and the relationship between the $In_{real}$, $In_{pre}$ (i.e., the intersections calculated with the simulation and NN methods $In_{real12}$ and $In_{pre12}$, simplified as $In_{real}$ and $In_{pre}$, respectively) and *Th* (i.e., the largest acceptable load). *BPL* and *UL* for various scenarios can be calculated based on $Load_{max}$, i.e., the load that maximizes the BP difference corresponding to various strategies over the range of interest. The determination of $Load_{max}$ depends on the load-versus-BP performance calculated with simulation and the wrong decision range. For better illustration, the determination of $Load_{max}$ in Scenario 5 is taken as an example, where both $In_{real}$ and $In_{pre}$ follow the situation in Fig. 2(b). The load-versus-BP curve with simulation is depicted as Fig. 2(b). The wrong decision range equals the interval between $In_{real}$ and $In_{pre}$. It is easy to infer that $Load_{max}$ corresponds to $Load_0$ when $In_{pre} \leqq Load_0$ ($Load_0$ refers the load threshold when BP performance of routing strategy with $cost_2$ starts to be larger than zero), while it equals to $In_{pre}$ when $Load_0 < In_{pre} \leqq Th$, i.e., $Load_{max}$ equals max ($Load_0$, $In_{pre}$) as shown in Table 3. Given the determined $Load_{max}$, the calculation of *UL* can be divided into two situations depending on the relative advantage of $cost_1$ and $cost_2$ at load = $Load_{max}$. Assuming that $cost_2$ shows superiority over $cost_1$ at $Load_{max}$, additional $S_a$ spectral slots are needed to achieve the same BP if using $cost_1$ instead of $cost_2$. The *UL* equals $S_a/(S + S_a)$, where *S* indicates the number of spectral slots for the superior strategy under the situation, i.e. $cost_2$, and $(S + S_a)$ refers to the number of spectral slots for the inferior one $cost_1$. If the situation is that $cost_1$ shows an advantage over $cost_2$ at $Load_{max}$, a similar definition can be applied to *UL* in terms of the number of transceivers and *UL* equals to $M_a/(M + M_a)$. $(M_a + M)$ and *M* indicate the number of transceivers to achieve the same BP with the sub-optimal routing strategy ($cost_2$) and optimal one ($cost_1$), respectively.

### 3.2. Impact of the observation range

Fig. 3 shows the impact of the observation range on the performance of the proposed scheme. With the variation of the observation range (i.e., BP range of interest), the distributions of tested cases and CDF of *E*, *BPL* and *UL* vary accordingly. The $Th_{BP}$ varies from 0.01, 0.05 to 0.1. As shown in Fig. 3(a), with the increase of $Th_{BP}$, the ratio of Scenario 1 remains unchanged while that of Scenario 7 decreases. As a result, the sum of ratios of Scenarios 1 and 7, i.e., the ratio of the error-free cases, decreases with the increasing $Th_{BP}$. This is because the scenario which the case belongs to depends on the relationship between the observation range and the intersection. According to the definitions, both Scenarios 1 and 7 have no intersection in the range of interest. However, there is no observed intersection for Scenario 1, while for Scenario 7 the intersection falls beyond the observation range. Therefore, for Scenario 1 the relationship is not affected by the variation of the observation range, while fewer cases belong to Scenario 7 as the intersection may fall into the observation range with an increase of the range. For other scenarios, their ratios vary with the increasing $Th_{BP}$. Nevertheless, the summed ratio of Scenarios 2 to 6 does not exceed 17% regardless of $Th_{BP}$, which means that error-free decision is achieved in a large portion (>83%) of the tested cases. As shown in Fig. 3(b), the *BPL* and *UL* induced by the wrong decision show the similar trend as *E*. Error-free ratio which is shown in Fig. 3(b), decreases with the larger $Th_{BP}$, which is consistent with Fig. 3(a). For most of the cases with non-zero decision error, the *E*, *BPL* and *UL* increase with the increasing $Th_{BP}$. The average values of {*E BPL UL*} of the tested cases are {2.00% 1.24% 0.29%}, {2.56% 3.16% 0.97%} and {2.83% 3.88% 1.19%} for $Th_{BP}$ of 0.01, 0.05 and 0.1, respectively. They slightly increase with the rising $Th_{BP}$.

With over 83% error-free ratio regardless of the observation range, the proposed scheme shows high accuracy of decision for the optimal

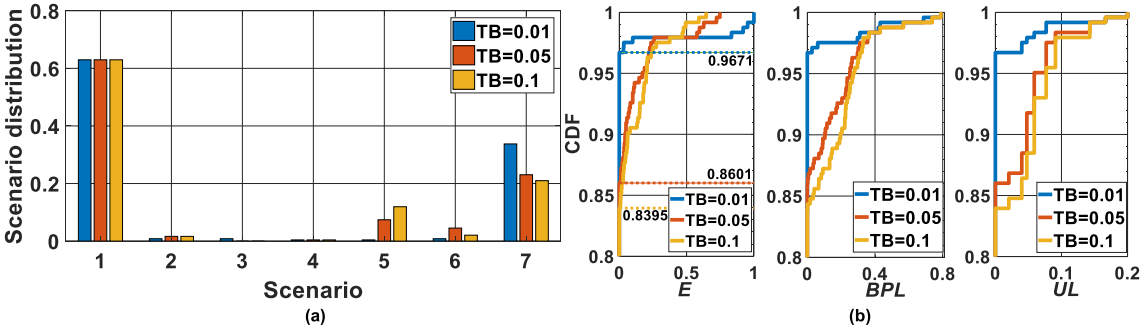


**Fig. 3.** (a) The scenario classification and (b) the cumulative distribution function (CDF) of the *E*, *BPL* and *UL* for 243 cases with different ranges of interest $Th_{BP}$ (i.e., "TB" in the legend). The error-free ratios for various $Th_{BP}$ are shown in the CDF of *E*.

routing strategy. The results also suggest the slight degradation of decision accuracy with the increase of observation range, i.e. the loosening of limitation of the worst acceptable BP performance. The variation of the *E*, *BPL* and *UL* when $Th_{BP}$ increases from 0.01 to 0.05 is larger than that in the case from 0.05 to 0.1. This suggests the accuracy of strategy decision is more sensitive to the range of interest when the range is relatively small.

### 3.3. Impacts of network parameters

The impacts of network parameters on the distributions of cases over the seven scenarios and the CDF of *E*, *BPL* and *UL* are presented in Figs. 4–8. According to the observation, the network parameters can be classified as two categories: an increased parameter that results in a right shift of the intersection (i.e., *N*, *M*) and that results in a left shift of the intersection (i.e., *D*, *S*, *R*). Due to the left/right shift of the intersection, the ratio of Scenario 1 decreases and that of Scenario 7 increases with the increase of *N* and *M*, while the increase of *D*, *S* and *R* results in a smaller ratio of Scenario 7 and a larger ratio of Scenario 1, which are shown in Figs. 4-8(a). This can be inferred from the definitions of Scenarios 1 and 7. It is observed the ratios of scenarios vary significantly with the change of network parameters, leading to the change of the optimal strategy in a remarkable number of tested cases. For example, when *D* increases from 4 to 8, 39.51% of all the tested cases change the optimal strategy from $cost_2$ to $cost_1$ throughout the range of interest as the cases transform from Scenario 7 to Scenario 1. This shows the high dynamics of the optimal strategy when changing network parameters, which implies that accurate decision-making with NN is of great importance for implementing adaptive routing strategy in optical DCNs.

As shown in Figs. 4-8(b), the error-free ratio (shown in CDF of *E*) generally increases with the rising of *D*, *S* and *R*, while it may decrease or increase for a larger *N* or *M*. The increase of error-free ratio is more obvious for a larger *D* or *R* and a smaller *S*. This indicates the proposed scheme performs better in DCNs with a larger *D* or *R* and a smaller *S*. Besides the error-free ratio, *E*, *BPL* and *UL* of the tested cases vary with the changed parameters. Despite of the variation, the measured *E*, *BPL* and *UL* are never larger than 3.0%, 4.0% and 1.2% in terms of their mean values, respectively. This again verifies the high accuracy of NN-assisted strategy decision with various network parameters.

In terms of the traffic characteristics, the high robustness with the traffic variation is revealed by the strategy decision scheme. The scope of traffic load under the investigation ranges from 0 to 540. Over this range, the ratio of error-free cases over all the tested cases reaches 83%. This, coupled with the average values no larger than 3.0%, 4.0% and 1.2% in the *E*, *BPL* and *UL* with the variation of *R* from 0.1, 0.5 to 0.9 (i.e., the average traffic capacity varies from 94 Gbps, 70 Gbps to 46 Gbps), suggests the proposed scheme is robust to the variation of traffic load.

It should be noted that the change of scenario distributions, *E*, *BPL* and *UL* caused by the network parameters is more remarkable compared to that induced by the observation range $Th_{BP}$. This is because both the intersections $In_{real}$ and $In_{pre}$ and the load range of interest *Th* vary with the varying parameters while only *Th* varies with the varying $Th_{BP}$. The increase of load range of interest *Th* with the same $Th_{BP}$ is due to the availability of more network resources (i.e., a larger *N*/*D*/*M*/*S*/*R*).

## 4. Conclusions

A NN-assisted decision-making scheme for routing strategy selection has been proposed to facilitate the adaptive routing in optical DCNs. The BP performance of candidate routing strategies is predicted by a trained NN for the arriving requests of any load in the optical DCN that is characterized by its networking parameters *N*, *D*, *M*, *S* and *R*. The candidate with the lowest BP is determined by the NN as the optimal routing strategy. To show the feasibility of the proposed scheme, its performance in the case of two-strategy decision for the transparent optical multi-hop interconnected DCN is evaluated and analyzed. Three metrics are proposed to assess the performance of the scheme over the range of interest, i.e., the decision error (*E*), the greatest BP and resource utilization losses (*BPL* and *UL*) due to the wrong decision. The impacts of the range of interest and the various network parameters on the

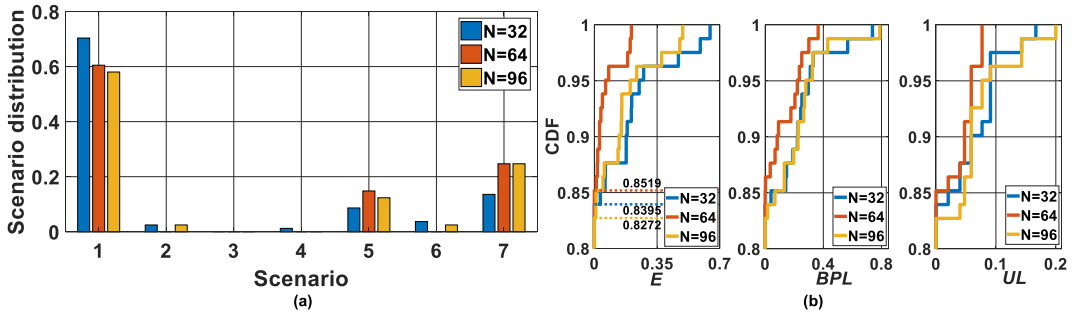


**Fig. 4.** (a) The scenario classification and (b) the CDF of *E*, *BPL* and *UL* for 243 cases with different numbers of racks *N*. The error-free ratios for various *N* are shown in the CDF of *E*.

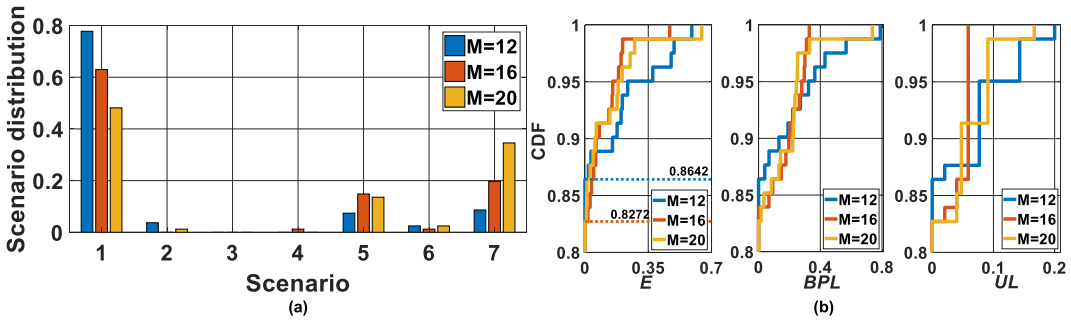


**Fig. 5.** (a) The scenario classification and (b) the CDF of *E*, *BPL* and *UL* for 243 cases with the different numbers of optical transceivers on each rack *M*. The error-free ratios for various *M* are shown in the CDF of *E*.

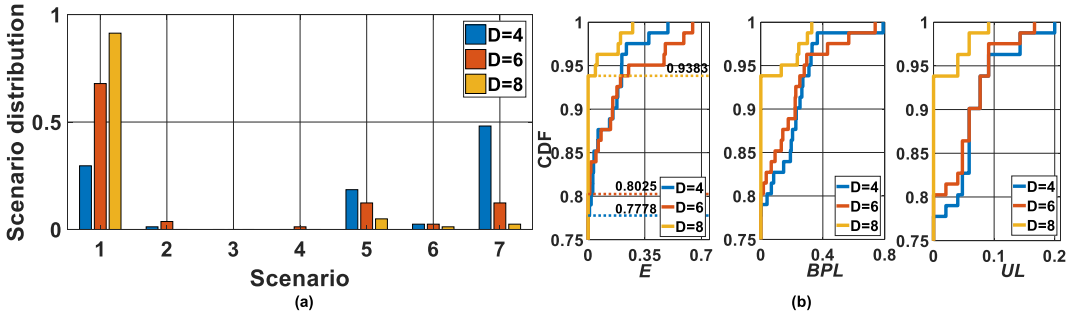


**Fig. 6.** (a) The scenario classification and (b) the CDF of *E*, *BPL* and *UL* for 243 cases with different degrees *D*. The error-free ratios for various *D* are shown in the CDF of *E*.

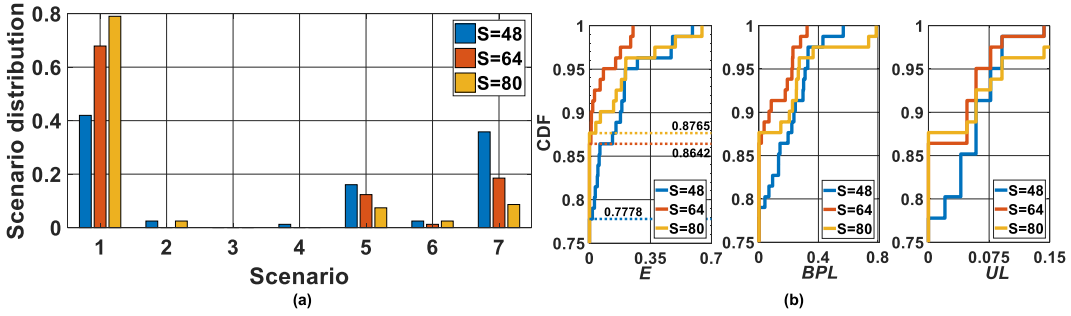


**Fig. 7.** (a) The scenario classification and (b) the CDF of *E*, *BPL* and *UL* for 243 cases with different numbers of spectral slots on each fiber link *S*. The error-free ratios for various *S* are shown in the CDF of *E*.

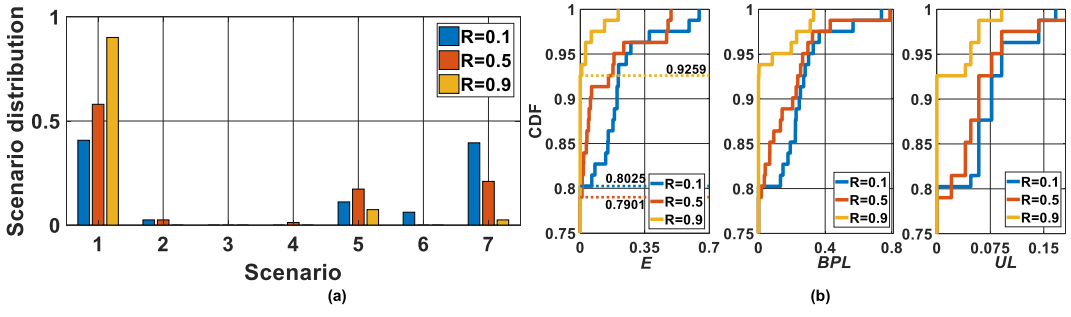


**Fig. 8.** (a) The scenario classification and (b) the CDF of *E*, *BPL* and *UL* for 243 cases with different ratios of the requests of 40Gbps/100 Gbps capacity *R*. The error-free ratios for various *R* are shown in the CDF of *E*.

performance are investigated.

The results demonstrate that with the increase of the range of interest and the loosening of the worst acceptable BP, the accuracy of the two-strategy decision-making only declines slightly, proving the robustness of the proposed scheme. The ratio of error-free cases over the tested cases (i.e. the error-free ratio) always exceeds 83% regardless of the range of interest. The average *E*, *BPL* and *UL* caused by the wrong decision when changing the network parameters are not larger than 3.0%,

4.0% and 1.2%, respectively. This verifies the feasibility of the proposed strategy decision-making scheme in the two-strategy scenario. Moreover, the error-free ratio generally increases with the larger connection degree $D$, spectral slot number $S$ and requests ratio of various capacities $R$. The improvement of error-free ratio is more obvious for a larger $D$ or $R$ and a smaller $S$, providing guidelines for the design of the optical DCNs with adaptive routing. It should be noted that in our study the NN model is trained with data set collected with simulation rather than the realistic data from the DCN operators which is often unavailable to the public. Nevertheless, it has been proven that the scheme can effectively learn from the simulation data and make reliable decisions for two routing strategies with the study. The scheme can be employed for the case of model training with realistic data without modification. The high accuracy and robustness of the proposed decision-making scheme imply that the smart adaptive routing is feasible which facilitates the network automation in optical DCNs.

Moreover, the proposed routing strategy decision scheme could be applied to any optical interconnection products with the intelligent network control and management. The workflow contains the training and provisioning phases. In the training phase the dataset is collected based on the data aggregated from the real-time status of the operator's network by the network controller. The training is performed offline and the trained model is then used for the online provisioning phase. The performance prediction assists in selection of the best routing strategy, which further informs the network controller.

## Author statement

Yuanyuan Hong: Conceptualization, Methodology, Software, Data curation, Investigation, Writing-Original draft preparation. Xuezhi Hong: Conceptualization, Methodology, Visualization, Validation, Writing-Reviewing and Editing. Jiajia Chen: Conceptualization, Methodology, Visualization, Supervision, Writing-Reviewing and Editing, Resources, Project administration.

## Declaration of competing interest

The authors declare that they have no known competing financial interests or personal relationships that could have appeared to influence the work reported in this paper.

## Acknowledgement

This work described in this paper was carried out with the support from National Natural Science Foundation of China under Grant 61550110240, National Natural Science Foundation of Zhejiang Province under Grant LQ20F010006, National Natural Science Foundation of Guangdong Province under Grant 2016A030313445, Swedish Foundation of Strategic Research, and Swedish Research Council.

## APPENDIX

**Table 3**
The Calculation Of Decision Error $E$, The BP Loss $BPL$ And Resource Utilization Loss $UL$ For Various Scenarios

Scenario 1:
$E = 0$
$BPL = 0$
$UL = 0$

Scenario 2:
$E = \frac{In_{pre}}{Th}$
$BPL = BPL(In_{pre})$
$UL = UL(In_{pre})$

Scenario 3:
$E = 1$
$BPL = BPL(Th)$
$UL = UL(Th)$

Scenario 4:
$E = \left[\frac{In_{real1}}{Th}, \frac{In_{real2}}{Th}\right]$
$BPL = BPL(Load_0)$
$UL = UL(Load_0)$

Scenario 5:
$$E = \begin{cases} \left[\frac{In_{real1} - In_{pre}}{Th}, \frac{In_{real2} - In_{pre}}{Th}\right] & \text{if } In_{pre} < In_{real1} \\ \left[0, \max\left(\frac{In_{real2} - In_{pre}}{Th}, \frac{In_{pre} - In_{real1}}{Th}\right)\right] & \text{if } In_{real1} < In_{pre} < In_{real2} \\ \left[\frac{In_{pre} - In_{real2}}{Th}, \frac{In_{pre} - In_{real1}}{Th}\right] & \text{if } In_{pre} > In_{real2} \end{cases}$$
$BPL = BPL(\max(Load_0, In_{pre}))$
$UL = UL(\max(Load_0, In_{pre}))$

Scenario 6:
$E = \left[\frac{Th - In_{real2}}{Th}, \frac{Th - In_{real1}}{Th}\right]$
$BPL = BPL(Th)$
$UL = UL(Th)$

Scenario 7:
$E = 0$
$BPL = 0$
$UL = 0$

[a] $Load_0$ refers the load threshold when BP performance of routing strategy with $cost_2$ starts to be larger than zero.

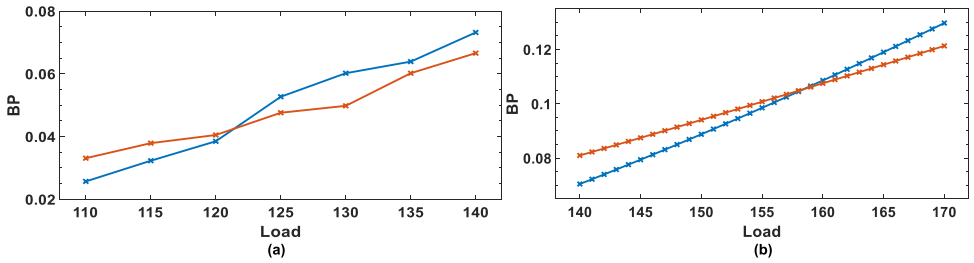


**Fig. 9.** The load-versus-BP performance curves calculated with the simulation and NN prediction. The load interval is set as 5 and 1 as example for simulation and NN, respectively. The parameter set {$N$, $D$, $S$, $M$, $R$} of the tested DCN case is {64, 6, 48, 12, 0.1}. The BP curves calculated with (a) simulation with the load interval of 5, (b) NN with the load interval of 1.

The seven possible scenarios of the calculation of $E$, $BPL$ and $UL$ are listed in Table 3. Note that the intersection with simulation is represented by a certain interval $[In_{real1}, In_{real2}]$ due to the limited resolution in load-versus-BP measurement, while the intersection with NN prediction is represented by a single value $In_{pre}$ in the table. In the actual operation, the intersections with simulation and NN are both positioned by certain load intervals and the corresponding BP performance. The load-versus-BP performance with NN is continuous enough to position the intersection in the small enough interval, e.g., an interval of 1, while the continuity of the BP curves with simulation is limited due to the stochastic nature of the simulation. The BP curves with load intervals of 1 and 5 are presented as examples for NN and simulation, respectively, as shown in Fig. 9. For simplicity, the intersection with NN is taken as a certain integer. To improve the reliability of the evaluation based on the calculated intersections, the intersection with simulation

is located by the interval [$In_{real1}$, $In_{real2}$], which satisfies that $BP_2$<$BP_1$ at $In_{real1}$ and $BP_2$>$BP_1$ at $In_{real2}$. The interval between the $In_{real1}$ and $In_{real2}$ is set to be a reasonable value (e.g., 10 in this work) to balance the accuracy and reliability of the intersection positioning. For the scenarios where the calculation of decision error $E$ relies on the intersection with simulation (i.e., Scenarios 4, 5 and 6), $E$ is obtained by averaging the minimal and maximum values calculated based on the interval [$In_{real1}$, $In_{real2}$].

## References


[1] Cisco, Cisco Global Cloud Index: Forecast and Methodology: 2016–2021 White Paper.

[2] J. Chen, Y. Gong, M. Fiorani, S. Aleksic, Optical interconnects at top of the rack for energy–efficient datacenters, IEEE Commun. Mag. 53 (8) (2015) 140–148.

[3] C. Karhris, I. Tomkos, A survey on optical interconnects for data centers, IEEE Commun. Surv. Tutorials 14 (4) (2012) 1021–1036.

[4] A. Wonfor, H. Wang, R.V. Penty, I.H. White, Large port count high-speed optical switch fabric for use within datacenters [Invited], J. Opt. Commun. Netw. 3 (8) (2011) A32–A39.

[5] N. Farrington, A. Forencich, G. Porter, P. Sun, J. Ford, Y. Fainman, G. Papen, A. Vahdat, A multiport microsecond optical circuit switch for data center networking, IEEE Photon. Technol. Lett. 25 (16) (2013) 1589–1592.

[6] N. Farrington, A. Andreyev, Facebook's data center network architecture, in: Proc. *Optical Interconnect. Conf. (OI), Santa Fe(America)*, 2013, pp. 49–50.

[7] Y. Yin, R. Proietti, X. Ye, C.J. Nitta, V. Akella, S.J.B. Yoo, LIONS: an AWGR-based low-latency optical switch for high-performance computing and data centers, IEEE J. Sel. Top. Quant. Electron. 19 (2) (2013) 3600409.

[8] K. Chen, A. Singla, A. Singh, K. Ramachandran, L. Xu, Y. Zhang, X. Wen, Y. Chen, Osa, An optical switching architecture for data center networks with unprecedented flexibility, IEEE Trans. Netw. 22 (2) (2014) 498–511.

[9] N. Terzenidis, M. Moralis-Pegios, G. Mourgias-Alexandris, K. Vyrsokinos, N. Pleros, High-port low-latency optical switch architecture with optical feed-forward buffering for 256-node disaggregated data centers, Opt Express 26 (7) (2018) 8756–8766.

[10] P. Bakopoulos, K. Christodoulopoulos, G. Landi, M. Aziz, E. Zahavi, D. Gallico, R. Pitwon, K. Tokas, I. Patronas, M. Capitani, C. Spatharakis, K. Yiannopoulos, K. Wang, K. Kontodimas, I. Lazarou, P. Wieder, D.I. Reisis, E.M. Varvarigos, M. Biancani, H. Avramopoulos, NEPHELE: an end–to-end scalable and dynamically reconfigurable optical architecture for application-aware SDN cloud data centers, IEEE Commun. Mag. 56 (2) (2018) 178–188.

[11] K. Sato, Realization and application of large–scale fast optical circuit switch for data center networking, IEEE J. Lightwave Technol. 36 (7) (2018) 1411–1419.

[12] K. Walkowiak, A. Kasprzak, M. Klinkowski, Dynamic routing of anycast and unicast traffic in elastic optical networks, in: Proc. *IEEE International Conf. Commun. (ICC), Sydney(Australia)*, 2014, pp. 3313–3318.

[13] M. Aibin, K. Walkowiak, Adaptive modulation and regenerator-aware dynamic routing algorithm in elastic optical networks, in: Proc. *IEEE International Conf. Commun. (ICC), London(UK)*, 2015, pp. 5138–5143.

[14] S. Yin, S. Huang, Y. Zhou, H. Huang, J. Zhang, W. Gu, Survivable routing, spectrum and waveband assignment strategy in cloud optical and data center network, Photonic Netw. Commun. 31 (3) (2016) 532–542.

[15] Y. Hong, X. Hong, S. He, J. Chen, Hybrid routing and adaptive spectrum allocation for flex–grid optical interconnect, J. Opt. Commun. Netw. 10 (5) (2018) 506–514.

[16] S. Troia, R. Alvizu, G. Maier, Reinforcement learning for service function chain reconfiguration in NFV-SDN metro-core optical networks, IEEE Access 7 (2019) 167944–167957.

[17] I. Martin, S. Troia, J.A. Hernandez, A. Rodrıguez, F. Musumeci, G. Maier, R. Alvizu, O.G. Dios, Machine learning-based routing and wavelength assignment in software-defined optical networks, IEEE T. Net. Serv. Man. 16 (3) (2019) 871–883.

[18] X. Chen, J. Guo, Z. Zhu, R. Proietti, A. Castro, S.J.B. Yoo, Deep-RMSA: a deep-reinforcement-learning routing, modulation and spectrum assignment agent for elastic optical networks, in: Proc. *43th Optical Fiber Communication Conf. (OFC), San Diego(America)*, 2018, pp. 1–3.

[19] L. Li, Y. Zhang, W. Chen, S.K. Bose, M. Zukerman, G. Shen, Naïve Bayes classifier-assisted least loaded routing for circuit-switched networks, IEEE Access 7 (2019) 11854–11867.

[20] R.N. Mysore, A. Pamboris, N. Farrington, N. Huang, P. Miri, S. Radhakrishnan, V. Subramanya, A. Vahdat, PortLand: a scalable fault-tolerant layer 2 data center network fabric, Comput. Commun. Rev. 39 (4) (2009) 39–50.

[21] Z. Zhu, S. Zhong, L. Chen, K. Chen, Fully programmable and scalable optical switching fabric for petabyte data center, Opt Express 23 (3) (2015) 3563–3580.

[22] T. Benson, A. Anand, A. Akella, M. Zhang, Understanding data center traffic characteristics, Comput. Commun. Rev. 40 (1) (2010) 92–99.

[23] K. Kanth, S. Prakash, Efficient utilization in processing rate of data on occurrence of a bursty traffic in a virtualization based cloud data center, Int. J. Sci. Res. Comput. Sci. Eng. Inf. Technol. (IJSRCSEIT) 3 (6) (2018) 138–142.

[24] W. Liu, Intelligent routing based on deep reinforcement learning in software-defined data-center networks, in: Proc. *International Symposium On Computers And Communications (ISCC), Vancouver(Canada)*, 2019.

[25] W. Liu, J. Li, Y. Wang, Z. Yang, D. Tang, L. Peng, Routing Method for Data Center Network Based on Deep Reinforcement Learning, CN 108401015 A(China), 2018.

[26] X. Chen, R. Proietti, H. Lu, A. Castro, S.J.B. Yoo, Knowledge-based autonomous service provisioning in multi-domain elastic optical networks, IEEE Commun. Mag. 56 (8) (2018) 152–158.

[27] L. Velasco, M. Klinkowski, M. Ruiz, V. López, G. Junyent, Elastic spectrum allocation for variable traffic in flexible grid optical networks, in: Proc. *Optical Fiber Communication Conf. (OFC), Los Angeles(America)*, 2012.

[28] W. Mo, C.L. Gutterman, Y. Li, S. Zhu, G. Zussman, D.C. Kilper, Deep-neural-network-based wavelength selection and switching in ROADM systems, J. Opt. Commun. Netw. 10 (10) (2018) D1–D11.

[29] K. Li, X. Wang, Y. Xu, J. Wang, Density enhancement-based long-range pedestrian detection using 3-D range data, IEEE T. Intell. Transp. 17 (5) (2016) 1368–1380.


**Yuanyuan Hong** was born in Guizhou, China, in 1991. She received the B.E. degree in information engineering and the Ph. D. degree in optical engineering from Zhejiang University in 2012 and 2018, respectively. She is currently a lecturer at Taizhou University. Her research interests include optical datacenter networks, routing and spectrum assignment algorithms.

**Xuezhi Hong** received the B.E. degree from Wuhan University, Wuhan, China, in 2006, and the Ph.D. degree from Zhejiang University, Hangzhou, China, in 2012. He was a postdoc at KTH Royal Institute of Technology, Stockholm, Sweden in 2016 and 2017. He is currently working as an Associate professor with South China Normal University, Guangzhou, China, working on visible light communication and positioning, optical fiber communication, and datacenter networks.

**Jiajia Chen** is a Professor in Chalmers University of Technology, Sweden. She received the bachelor's degree from Zhejiang University, China in 2004, and Ph.D. from KTH Royal Institute of Technology, Sweden in 2009. She and her group have made advances in optical network architecture design along with the supporting transmission techniques and resource allocation strategies, which greatly improve capacity, reliability, energy efficiency and cost efficiency in access, core and data center networks. She has been sharing her knowledge with the technical community with many peer-reviewed journal articles, conference papers, invited talks (200+ publications to-date) and 10 patent applications. She has organizing several IEEE international conferences in the field and serving on technical program committees, including OFC (Subcommittee Chair 2019), ECOC, Globecom (Symposium Co-Chair 2020), ICC, etc.